IMPROVED INTEGRATION-RESET CONTROLLED SINGLE PHASE UNITY-POWER-FACTOR BOOST RECTIFIER WITH LOWER DISTORTION

DORIN CISMASIU
Facultatea de Inginerie
Universitatea "Lucian Blaga" din Sibiu
550025 Sibiu, Str. Emil Cioran Nr.4
ROMANIA

VIOREL POPESCU,DAN LASCU
Fac. de Electronică şi Telecomunicaţii
Universitatea Politehnică din Timişoara
3000223 Timişoara Bd. V. Pârvan Nr.2
ROMANIA

Abstract:- This paper presents an improved integration method to realize single phase power factor correction in continuous conduction mode by adding a ripple compensation network comprised of two resistors to the basic integration control circuitry. This method effectively reduces the total harmonic distortion (THD) in the input current. The method is easy to implement. Theoretical analysis is given in detail. Experimental results demonstrate the validity of the approach.

Key-Words:- active power factor correction, integration-reset control, boost rectifier.

1 Introduction

In accordance with the operation mode of the power stage, power factor corrected rectifiers (PFC) may be divided into three categories:
Continuous Conduction Mode (CCM), Critical Conduction Mode (CrCM) and Discontinuous Conduction Mode (CCM). For high power applications (above one kilowatts), CCM operated rectifiers are preferred due to their low conducted noise, low conduction losses in the semiconductor switches and inductors, and low inductor core losses. Average mode control and peak current control are often used to control CCM operated rectifiers. The average current control method has demonstrated lower input current harmonic than the peak current control. These control methods are complex because both of them require a stabilization ramp for their current control loops. Furthermore, a sensor of the rectified AC voltage is used to provide a current reference and a multiplier is used to scale the reference so that it reflects the output current and voltage requirements. In order to simplify the control scheme, several control methods have been proposed [2-5]. The nonlinear-carrier-control [4] in the first time eliminated the need of a multiplier. The integration control [2,6] employs integrators with reset to control the CCM operated rectifiers and eliminates the need of the multiplier.
Similar to the peak current control method, the integration peak current controlled rectifiers also exhibit input current distortions. For integration controlled Boost rectifiers several sources of input current distortion are [2] :
(1). Input inductor current ripple that causes the average current to deviate from the ideal sinusoidal waveform.
(2). Partially discontinuous operation of the input inductor current.
(3). The 100Hz ripple at the output is fed into the output of the voltage error amplifier.
The integration control method can be improved to reduce the input current distortion by adding a simple ripple compensation network . With this method, the distortion source (1) is eliminated and source (2) is significantly decreased by reducing the subinterval where the converter operates in DCM. In Section 2, the scheme of the basic integration controlled boost rectifier is reviewed. In Section 3, the compensation method and its function in the converter is detailed.
Experimental results are provided to demonstrate the validity of the theory in Section 4. Finally, a conclusion is given in Section 5.
Capital letters are used for quantities associated with steady-state; lower letters represent time-variant variables; a quantity upperlined is the average of the quantity in each switching cycle.

2 Basic integration controlled boost PFC

A typical single phase PFC is comprised of a diode bridge in series with a DC-DC converter.
Fig. 1 shows the basic schematic of the integration controlled boost PFC rectifier, realized through an integrator with reset.

For PFC applications, the control goal of the DC-DC converter is

$$\bar{i}_g = \frac{V_g}{R_e} \tag{1}$$

where R_e is the emulated resistance V_g is the input voltage and i_g the input current of the DC-DC converter.

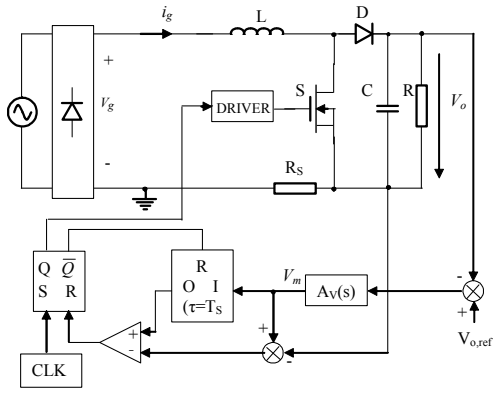

Fig. 1. The schematic of the integration controlled boost PFC rectifier

During the quasi-steady state,a DC-DC converter satisfies the following equation

$$\frac{V_o}{V_g} = M(D) \tag{2}$$

where M(D) is the conversion ratio of the DC-DC converter. Combination of equation (1) and (2) leads to the general PFC control function

$$R_S \bar{i}_g = \frac{V_m}{M(D)} \tag{3}$$

where $V_m = \frac{R_S V_o}{R_e}$ and R_s is the equivalent current sensing resistance.

For boost converter, the conversion ratio is $M(D) = \frac{1}{1-D}$. The general PFC control function becomes

$$R_s \bar{i}_g = V_m (1-D) \tag{4}$$

Assuming current ripple is small, the peak input inductor current i_{Lpk} approximately equals the average input current $\bar{i}_g$. Therefore, the peak current is sensed for the control. The equation (4) can be reorganized as

$$R_s i_{Lpk} = V_m - V_m D \tag{5}$$

In Fig.1 this equation is achieved as follows:

$$V_m - R_s i_{Lpk} = \frac{V_m}{\tau} DT \tag{6}$$

where τ is the integration time constant, V_m is the output of the voltage loop error amplifier and T is the switching period. By setting $\tau = T$, the equation (6) will be the same as the equation (5). With this peak current control, input peak current is proportional to the input voltage that is given by

$$\bar{i}_{Lpk} = \frac{V_m}{R_s V_o} V_g \tag{7}$$

The following conclusion: is drawn from the above analysis:

First, when the current ripple is small enough comparing with average current, the peak current approximately equals the average current, the control goal of PFC (see equation (1)) is achieved. However, when the input current is smaller, the current ripple will cause larger distortion. The average inductor current (which is also the average input current $\bar{i}_g$ for boost converter) equals the peak inductor current minus the current ripple. Therefore, the average input current is given by

$$\bar{i}_g = \frac{V_m}{R_s V_o} V_g - \frac{1}{2}\frac{T}{L} V_g \left(1 - \frac{V_g}{V_o}\right) \tag{8}$$

Second, the equation (8) is generated based on the assumption that the converter operates in CCM. In reality, when the input current is near zero or the load is light, the converter will operate in discontinuous mode during certain region.

During DCM interval, the conversion ratio is not a unique function of duty cycle; it is also a function of switching period T, inductance L, load resistance, input and output voltage ratio M_g, i.e. $\frac{V_o}{V_g} = f(T, L, R, M_g, D)$. The average input current during the DCM interval will also related to these parameters such as T, L, R, M_g, D and is no longer proportional to the input voltage. A typical average inductor current waveform during the half line cycle is shown in Fig.2.

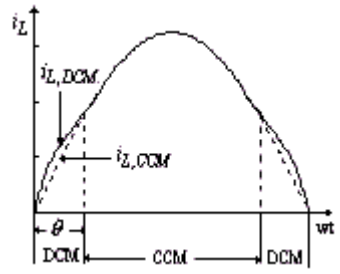

Fig. 2. Typical average inductor current during half line cycle for integration controlled boost PFC rectifiers

Fig. 2 shows the average inductor current in a half line cycle. The converter operates in CCM when $\theta \le \omega t \le \pi - \theta$ and DCM for the rest of the half cycle. The larger the DCM conduction angle θ is, the greater the distortion is. The improved

integration control will eliminate or reduce these distortions.

3 The improved integration controlled boost PFC rectifiers

3.1 Ripple compensation

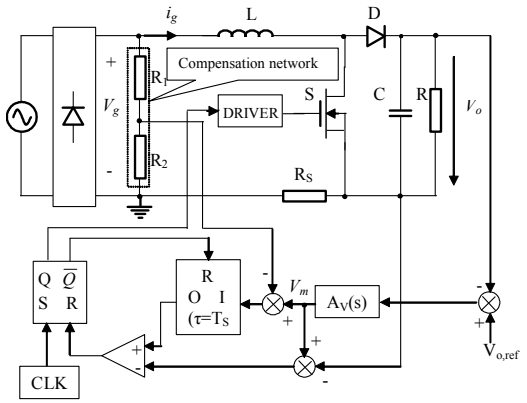

Fig. 3. The schematic of the improved integration controlled boost PFC rectifier

By adding a compensation network and a summer, the control equation (6) is modified as

$$V_m - R_s i_{Lpk} = \frac{V_m - kV_g}{T} DT \tag{9}$$

where $k = \dfrac{R_2}{R_1 + R_2}$

Following the same procedure, we can get the average inductor current as follows:

$$\bar{i}_g = \frac{V_m V_g}{R_s V_o} + \left(\frac{k}{R_s} - \frac{T}{2L} \right) V_g D \tag{10}$$

the average inductor current will be

$$\bar{i}_g = \frac{V_m V_g}{R_s V_o} \tag{11}$$

if $k = \dfrac{R_s T}{2L}$

From equation (11), the average input current will be exactly proportional to the input voltage. Thus, the distortion due to inductor current ripple is eliminated.

3.2 Reduction of DCM region

Another advantage of the compensation is to reduce the subinterval in each half line cycle where the converter operates in DCM, i.e. the proposed compensation network reduces θ as shown in Fig. 4

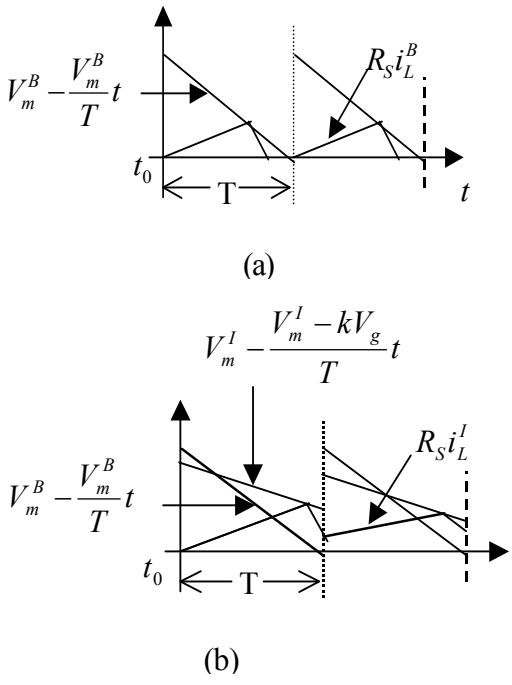

Fig. 4. The control scheme comparison between the basic and improved integration control (a). The basic integration control. (b) The improved integration control

In Fig. 4 (a) and (b), V_m^I and V_m^B are the output of voltage error amplifier for the basic and improved integration controlled rectifiers respectively. Likewise, i_L^i and i_L^B are the inductor currents of converters respectively, in the improved integration control and the basic integration control.

Suppose the two converters operate in the same conditions (i.e. same input voltage and load).

When $t < t_o$, we assume that both the converter operate in DCM. In most case, the slope of the compensation loop for the improved integration controlled converter is smaller than that of the basic integration controlled converter, i.e.

$$\frac{V_m^I - kV_g}{T} < \frac{V_m^B}{T}$$

Fig. 4 shows that the inductor current will go from DCM into CCM earlier for improved integration control comparing with the basic integration control. In other words, the improved method leads to smaller θ, thus converter operates in smaller DCM region. Therefore, the improved method reduced the distortion caused by the partial discontinuous conduction mode.

This is verified by comparing the DCM conduction angle θ for the basic and improved integration controlled boost PFC.

3.2.1 The derivation of DCM conduction angle θ for improved integration control

setting $k = \frac{R_s T}{2L}$, the (9) equation become

$$V_m - R_s i_{Lpk} = \left(V_m - \frac{R_s T}{2L} V_g \right) D \tag{12}$$

If the converter operates in DCM, the inductor peak current is

$$i_{Lpk} = \frac{V_g}{L} DT \tag{13}$$

Combining (12), (13) yields

$$D_{DCM} = \frac{1}{1 + \frac{L_n}{V_m}} V_{g,n} \tag{14}$$

Where D_{DCM} is the duty cycle when converter operates in the DCM subinterval; L_n is normalized inductance; $V_{g,n}$ is the normalized input voltage.

$$L_n = \frac{R_s T V_o}{2L} \tag{15}$$

$$V_{g,n} = \frac{V_g}{V_o} = \frac{V_{gM} |\sin \omega t|}{V_o} \tag{16}$$

If the boost converter operates in CCM, the duty ratio is

$$D_{CCM} = 1 - \frac{V_g}{V_o} = 1 - \frac{V_{gm} |\sin \omega t|}{V_o} \tag{17}$$

At the CCM and DCM boundary,($\omega t = \theta$), D_{CCM} should equal to D_{DCM} , which gives

$$\theta = a \sin \left[\frac{1}{M_g} \left(1 - \frac{V_m}{L_n} \right) \right] \tag{18}$$

Assuming the average input power equals output power during each line cycle and power factor equals unity,

$$\frac{V_{gM}}{\sqrt{2}} \bar{i}_{g,rms} = P_o = P_{o,n} P_M \tag{19}$$

where $P_{o,n}$ is the normalized output power;

$P_M = \frac{V_o^2}{R}$ is the rated power; R is rated load.

For the first order approximation, the input average input current can be expressed by equation (11) no matter what kind of mode the converter operates. From equation (11), we have

$$\bar{i}_{g,rms} = \frac{1}{\sqrt{2}} \frac{V_m}{R_s} \frac{V_g}{V_o} = \frac{1}{\sqrt{2}} \frac{V_m}{R_s} M_g \tag{20}$$

From (19), (20) yields

$$V_m = \frac{2 R_s V_o}{R} \frac{P_{o,n}}{M_g^2} \tag{21}$$

Substituting (21) into (18), we get

$$\theta^I = a \sin \left[\frac{1}{M_g} \left(1 - \frac{4 P_{o,n}}{M_g^2 R} \frac{L}{T} \right) \right] \tag{22}$$

3.2.2 The derivation of DCM conduction angle θ for basic integration control

Assuming the input power equals the output power during one line cycle, yields

$$\frac{1}{2\pi} \int_0^{2\pi} V_g \bar{i}_g d\omega t = P_{o,n} P_M \tag{23}$$

where $\bar{i}_g$ is determined by equation (8).

We have

$$V_m = \frac{R_s V_o T}{2L} + \frac{2 R_s}{M_g^2} - \frac{4}{3\pi} \frac{V_{gM} T R_s}{L} \tag{24}$$

Following the similar procedure, we can get the DCM conduction angle θ^B

$$\theta^B = a \sin \left[\frac{1}{M_g} \left(\frac{1}{2} - 2 \frac{L}{T} \frac{P_{o,n}}{R M_g^2} + \frac{4}{3\pi} M_g \right) \right] \tag{25}$$

Fig.5 shows the DCM conduction angle θ_I , θ_B vs. the normalized load for the improved and the basic integration controlled PFC boost rectifiers respectively. It is clear that in most case, the DCM conduction angle θ for improved integration control is smaller than that of the basic integration control. Therefore, the distortion of the input current should be lower.

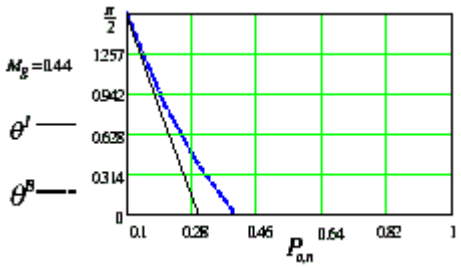

(a)

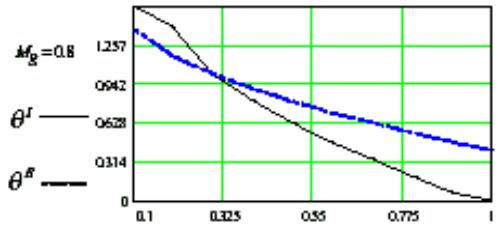

(b)

Fig. 5 The DCM conduction angle θ^I and θ^B vs. normalized load.Fig. 2 shows that the converter operates in completely CCM if θ=0 . Likewise, the

converter operates in completely DCM when $\theta=\pi/2$. By setting DCM conduction angle $\theta=0$ and $\theta=\pi/2$ for equation (22) and (25), the boundary condition equations (26) and (27) for the improved and the basic integration control are obtained respectively.

$$\begin{cases} \theta^I = 0 \quad CCM/CCM\ \&\ DCM\ boundary \\ \qquad P^I_{o,n1} = \dfrac{RT}{4L} M_g^2 \\ \theta^I = \dfrac{\pi}{2} \quad CCM\ \&\ DCM/DCM\ boundary \\ \qquad P^I_{o,n2} = \dfrac{RT}{4L} M_g^2 \left(1 - M_g\right) \end{cases} \tag{26}$$

$$\begin{cases} \theta^B = 0 \quad CCM/CCM\ \&\ DCM\ boundary \\ \qquad P^B_{0,n1} = \dfrac{1}{2} \dfrac{\frac{1}{2} + \frac{4}{3\pi} M_g}{L} TRM_g^2 \\ \theta^B = \dfrac{\pi}{2} \quad CCM\ \&\ DCM/DCM\ boundary \\ \qquad P^B_{o,n2} = \dfrac{1}{2} \dfrac{\frac{1}{2} + \frac{4}{3\pi} M_g - M_g}{L} TRM_g^2 \end{cases} \tag{27}$$

Fig. 6 shows the CCM and CCM&DCM boundary for both control methods. The CCM is obviously enlarged for improved integration control.

4 Experiment Verification

A 250W prototype boost PFC is built in order to verify the theoretical analysis.

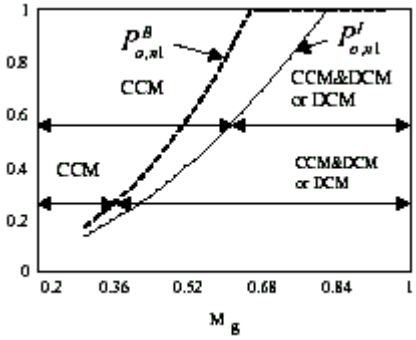

Fig. 6. The CCM and CCM&DCM boundary for improved/basic integration control

Input voltage ranges 85V ÷ 270Vrms; V_o =385V, f=100kHz; L= 1mH

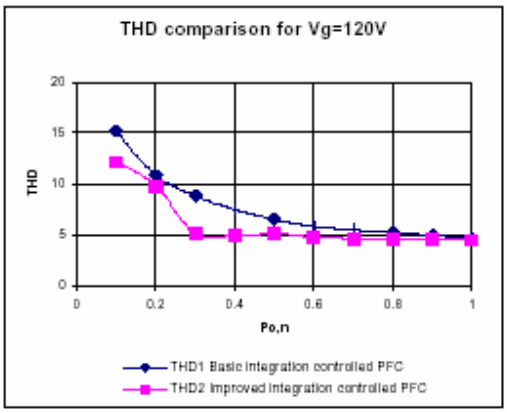

(a).

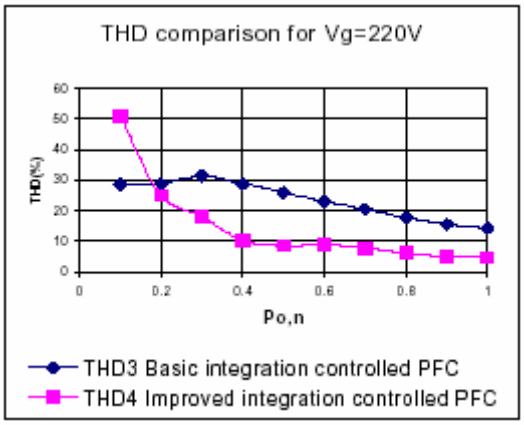

(b)

Fig. 7 The THD comparison between the improved/basic integration controlled boost PFC rectifier

The THD is very close for both converters when the power approaches the full load. However, at the light and medium load, the THD is significantly reduced using improved integration control. This is further verified by the measured input current waveforms. Fig. 7 shows the waveforms of the input current when input voltage is 230Vrms and the output power is 100w(40% of full load). The experiments demonstrated that the proposed method not only reduces the distortion when inductor operates on CCM mode, but also enlarges the CCM region.

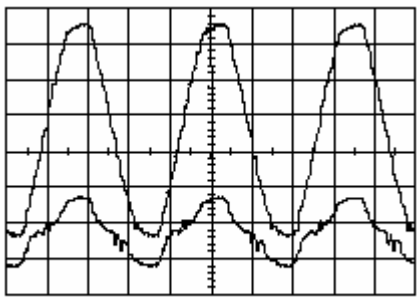

(a)

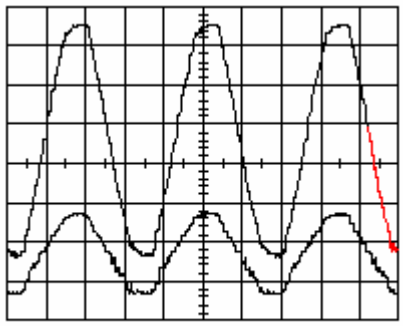

(b)

Fig. 8 Line voltage and input current waveforms for an experimental 250W power factor corrected rectifier using basic (a)/improved (b) integration control respectively

Experimental conditions: Vg,rms =230V , Pout=100W (40% of full load). Top curve: input

AC voltage, 100V/div, 5ms/div. Bottom curve: input AC current, 1A/div., 5ms/div

5 Conclusion

Integration control method enables simple, low cost, stable power factor control of continuous conduction mode rectifiers. A simple compensation network adds following advantages:

- Eliminate the input current distortion caused by current ripple;
- Has lower THD for light and medium load by significant reducing the DCM conduction angle θ;
- Easy to implement, only two resistors needed to add into the circuitry;

The disadvantage is the need to sense the input voltage. However, in practice, the input voltage is required to compensate the input RMS variation anyway. The theoretical analysis is verified by the experimental results.

REFERENCES

[1]. Redl, R.; Erisman, B.P. "Reducing Distortion in Peak-Current-Controlled Boost Power-Factor-Correctors". *APEC '94*.

[2]. Lai, Z.; Smedley, K.M. "A family of powerfactor-correction controllers". *APEC'97. New York, NY, USA: IEEE, 1997*. p.66-73 vol.1

[3]. Gegner, J.P.; Lee. C.Q. "Linear Peak Current Mode Control: A Simple Active Power Factor Correction Control Technique For Continuous Mode". *PESC 96 Record. New York, NY, USA: IEEE, 1996*. p.196-202 vol.1.

[4]. Maksimovic, D. Nonlinear-Carrier Control For High Power Factor Boost Rectifiers", *IEEE Transactions on Power Electronics*, vol.11, (no.4), 0IEEE, July 1996. p.578-84.

[5]. Maksimovic, D. Design of the clamped-current high-power-factor boost rectifier. *IEEE Transactions on Industry Applications*, vol.31, (no.5), Sept.-Oct. 1995. p.986-92.

[6]. Lai, Z.; Smedley,K.M. "A General Constant Frequency Pulse-Width Modulator and Its Applications". *IEEE Transactions on Circuits and Systems I: Fundamental Theory and Applications*, vol 45.(no.4), IEEE, April, 1998.P.386-96.